



UV-induced photolysis of polyurethanes†

Cite this: *Chem. Commun.*, 2021, **57**, 2911

Received 8th January 2021,
Accepted 8th February 2021

DOI: 10.1039/d1cc00124h

rsc.li/chemcomm

Waste production associated with the use of non-degradable materials in packaging is a growing cause of environmental concern, with the polyurethane (PU) class being notorious for their lack of degradability. Herein, we incorporate photosensitive *ortho*-Nitrobenzyl units into PUs to achieve controllable photodegradability. We performed their photolysis in solution and thin films which can inform the design of degradable adhesives.

Polyurethanes (PUs) are employed in a wide variety of applications, ranging from industrial products such as shoe soles, wheels, construction, packaging, and adhesives^{1,2} to drug delivery as well as for *in vitro* and *in vivo* biocompatibility studies for enzymatic, tissue and cellular responses to the material.^{3–8} The Bayer chemical company greatly contributed to expand the types of PUs in industry, particularly with the invention of the diisocyanate polyaddition technique, thus leading to the establishment of the PU industry in 1937.⁹ The properties of PU resulting from the reaction of polyols and isocyanates depend mainly on the nature of starting compounds they are made of.² For example, long and flexible polyols usually generate soft elastic polymers, while highly crosslinked polymers lead to rigid and hard materials.¹⁰ Despite their outstanding mechanical, physical, and chemical

properties, PUs' main challenge remains achieving degradability. With such extensive applicability, this gives rise to high levels of waste unable to be recycled. High temperature treatment is the most used technology for the waste management of PUs,¹¹ however combustion is not only energy intensive, but also generates harmful gas emissions.¹² On the other hand, light can trigger degradation and is a powerful tool as it allows for spatial and temporal control.

ortho-Nitrobenzyl (*o*NB) derivatives are commonly used in photochemistry and -biology owing to their capability to cleave upon light irradiation.^{13–17} Indeed, under ultraviolet (UV) light, *o*NB moieties undergo a Norrish II type reaction, leading to the formation of a nitroso compound and the release of a carboxylic acid.^{18–22} Herein, we incorporate photodegradable moieties into PU polymer chains (Scheme 1). A step-growth polymerization process with *o*NB-containing dialcohol and diisocyanates readily allows for the insertion of these photodegradable moieties into every second monomer unit. After investigating the light-induced degradation of the photosensitive monomer, the polymer photolysis was performed in diluted conditions as well as on thin films. An *o*NB-based dialcohol (Scheme 1, orange) was synthesized via a 3-step procedure (Fig. 1, experimental procedures are available in the ESI†). The first step consists of the formation of *tert*-butyl 2-(4-acetyl-2-methoxyphenoxy)acetate from acetovanillone, followed by a nitration step to afford the carboxylic acid **3** and a final reduction driven by BH₃, allowing for the formation of the *o*NB dialcohol monomer **4** (Fig. 1). Due to the presence of boric acid as a by-product, a purification through amberlite 743 was carried out to obtain the *o*NB dialcohol in high purity. The ¹H and ¹³C NMR spectra, as well as mass spectra of the precursors, are available in the ESI† (Fig. S4–S12). In order to verify the *o*NB cleavage when exposed to near visible light (close to 400 nm), its physicooptical properties must be assessed. Stationary UV/Vis absorption studies of the *o*NB dialcohol precursors were performed in acetonitrile at 25 °C (Fig. 1). The addition of the *tert*-butyl moiety (Fig. 1, **1** → **2**) leads to a significant increase of absorbance in the region around 330 nm. However, both the acetovanillone and its ester derivatives exhibit no absorbance at

^a Centre for Materials Science, School of Chemistry and Physics, Queensland University of Technology (QUT), 2 George Street, Brisbane, QLD 4000, Australia. E-mail: christopher.barnerkowollik@qut.edu.au, j.blinco@qut.edu.au

^b Institute of Physical Chemistry, Karlsruhe Institute of Technology (KIT), Fritz-Haber-Weg 2, 76131 Karlsruhe, Germany. E-mail: andreas.unterreiner@kit.edu

^c Ivoclar Vivadent AG, Bendererstrasse 2, 9494 Schaan, Liechtenstein

^d Institute of Nanotechnology (INT), Karlsruhe Institute of Technology (KIT), Hermann-von-Helmholtz-Platz 1, 76344 Eggenstein-Leopoldshafen, Germany

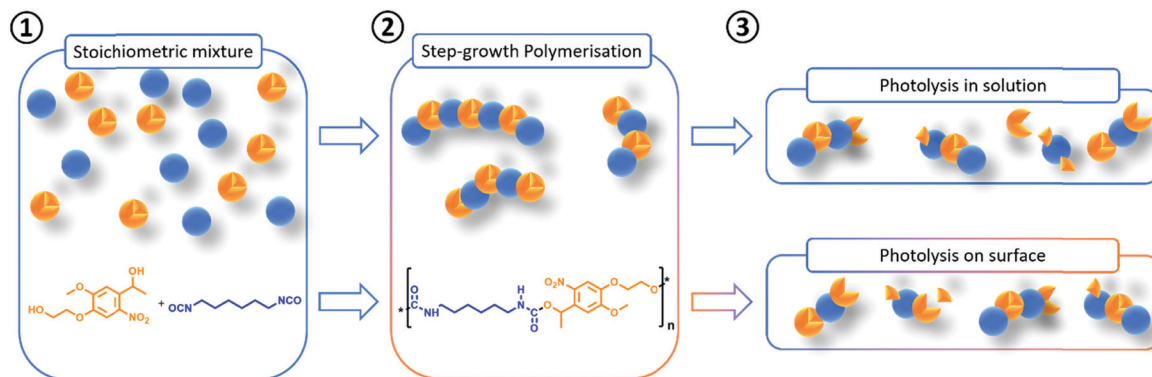
^e Institute of Organic Chemistry, Heidelberg University, Im Neuenheimer Feld 270, 69120 Heidelberg, Germany

^f Center for Advanced Materials, Heidelberg University, Im Neuenheimer Feld 225, 69120 Heidelberg, Germany

^g Centre for a Waste-Free World, Queensland University of Technology (QUT), 2 George Street, Brisbane, QLD 4000, Australia. E-mail: christopher.barnerkowollik@qut.edu.au

† Electronic supplementary information (ESI) available. See DOI: 10.1039/d1cc00124h

‡ These authors contributed equally.



Scheme 1 Overall scheme of the step-growth polymerisation of *o*NB dialcohol and hexamethylene diisocyanate (HDI) followed by the photolysis performed in solution, solvent-free and on thin film. The step-growth polymerisation of an *o*NB-dialcohol (in orange) with hexamethyl diisocyanate (HDI, in blue) is performed from a stoichiometric solution. The photolysis of the resulting polymers is then achieved in solution or in thin films.

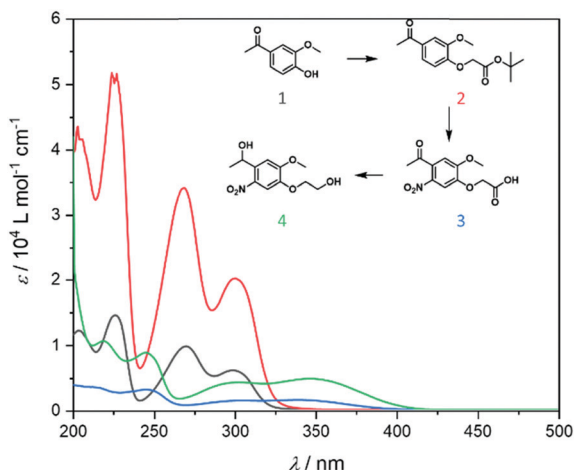


Fig. 1 Ultraviolet-visible absorbance spectra of the *o*NB-dialcohol and its intermediates, (1) acetovanillone, (2) *tert*-butyl 2-(4-acetyl-2-methoxyphenoxy)acetate, (3) 2-(4-acetyl-2-methoxy-5-nitrophenoxy)acetic acid, (4) 1-(4-(2-hydroxyethoxy)-5-methoxy-2-nitrophenyl)ethan-1-ol.

350 nm or higher. Insertion of a nitro group induces an absorbance band around 400 nm. This feature is of key importance, as the transmittance of typical plastic materials is usually below 350 nm.²³ The final reduction step (Fig. 1, 3 → 4) further increases the absorbance. As a result, the *o*NB dialcohol absorbs light mainly below 400 nm, an essential feature for degrading coloured polymeric material. It is expected that the photolysis of the *o*NB moiety occurs between 350 and 400 nm, according to the newly introduced absorption band in this region.

To proceed with the step-growth polymerization of the dialcohol *o*NB with a diisocyanate, we used dibutyl tin dilaureate (DBTL) as a catalyst. The nucleophilic addition on the C=N bond is eased by the polarization of the isocyanate or the hydroxyl moieties. The addition of an equimolar amount of hexamethylene diisocyanate (HDI) and a catalytic amount of DBTL led to the formation of *o*NB-based PU after 2 to 20 min at 70 °C via a step-growth polymerization process. The resulting polymers were analysed via size exclusion chromatography (SEC), the traces obtained with UV detection at 360 nm are displayed in Fig. 2. As expected from a step-growth process, each

SEC trace is a sum of Gaussian curves resulting from the successive addition of monomer units (Fig. S23 and S24, ESI[†]).

In addition, the polymers obtained via step-growth polymerization after 2 to 20 min were analysed by SEC-ESI-MS. The successive addition of *o*NB-dialcohol and hexamethyl diisocyanate can be assessed by the increase of the *m/z* value of 257.09 and 168.09, corresponding to their respective exact masses divided by the charge (Fig. S26, ESI[†]). Additionally, when the last monomer added is hexamethyl diisocyanate, an amine end-group has been observed. We assume that during the ESI[†] process, the reaction of the isocyanate group with water forms an unstable carbamic acid intermediate, which decomposes to an amine releasing carbon

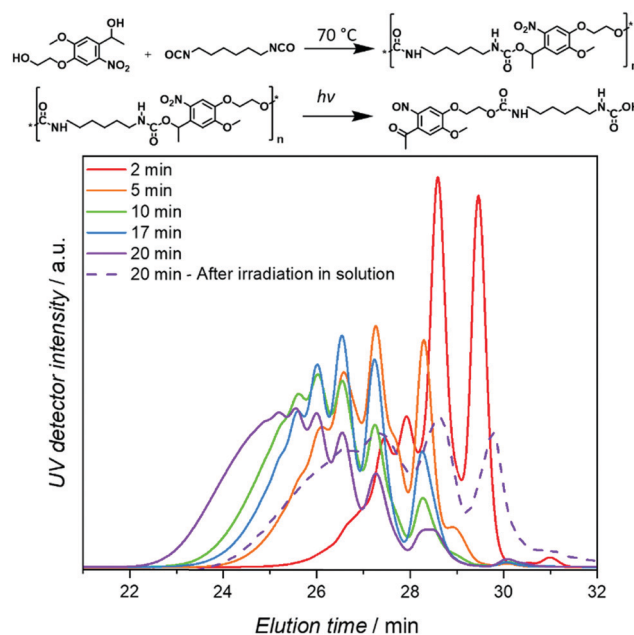


Fig. 2 Top: Reaction scheme of the step-growth polymerization of *o*NB-dialcohol with hexamethylene diisocyanate (HDI) and its photolysis. Bottom: Size Exclusion Chromatography (SEC) traces of PUs after 2 to 20 min reaction at 70 °C and the spectra obtained after irradiation at 365 nm in a solvated environment. Ultraviolet detection at 360 nm; the curves were normalized to the same area.

dioxide. As a result, the increase of m/z of 142.11 instead of 168.09 due to the presence of an amine instead of an isocyanate end-group (Scheme S4, ESI†).

The understanding of the *o*NB cleavage mechanism is essential from the perspective of a multi-component-material used in an industrial environment. Indeed, to achieve the effective photodegradation of an *o*NB-based adhesive material, side-reactions must be avoided in favour of the photolysis process. The photolysis of nitrobenzyl compounds studied by electron paramagnetic resonance has been reported in the literature.^{24–27} EPR spectra of many *para*-substituted compounds have been studied and the mechanism of the splitting patterns is well understood,^{24,25} but to date few examples involving *ortho*-substituted compounds are described.^{26,27} To the best of our knowledge, all the examples with *o*NB moiety describe the photolysis in an aqueous environment.

To allow for further in-depth analysis via SEC and SEC-ESI-MS, the polymer formed from nitrobenzyl-based monomeric unit must be soluble in organic solvents. Even though the splitting pattern of *ortho*-Nitrobenzyl relies on the position of the main substituent group in relation to the $-\text{NO}_2$ group on the aromatic ring, the observed EPR spectrum is also dependant on the experimental conditions (*e.g.* solvent). The light-induced degradation of the *o*NB moiety in organic solvents (here CDCl_3) leads to the heterolytic cleavage of the $\text{N}=\text{O}$ bond, thus generating free radicals on both the N and one of the O atoms. The abstraction of a proton from the N by the O atom induces the transfer of a free radical to the carbon holding the secondary alcohol function (Fig. 3①).

Nevertheless, radical formation represents only the first step of the degradation process. To achieve an in-depth understanding of the overall degradation of *o*NB dialcohol to a ketone-nitroso compound, FT-IR and $^1\text{H-NMR}$ spectroscopy were used. On the one hand, the infrared spectrum provides insight into changes of functional groups before and after irradiation (Fig. S16, ESI†) with the observation of a carbonyl band after irradiation. On the other hand, $^1\text{H-NMR}$ indicates a change in the environment of the protons on the methyl group in α -position to the carbonyl (Fig. S15, ESI†). Both techniques confirm the pathway proposed (Fig. 3) and thus $^1\text{H-NMR}$ can be used as a reliable quantitative technique for photolysis study.

To gain insights on the degradation efficiency of the *o*NB-dialcohol and in order to determine the relation between physicooptical properties and degradation efficiency, blue visible or UV light is used. A nanosecond pulsed laser with a tuneable light source allows the space and time-controlled irradiation of samples in solution. Tunable laser experiments with a constant photon count at specific wavelengths were carried out. Detailed descriptions of the setup and relevant calculations are available in the ESI† (Page S4).^{28–30} Our team previously reported discrepancies between photochemical reactivity and photon absorbance of photochemical moieties. These differences are typically captured in action plots.²⁸ The action plot of the *o*NB compound **4** (Fig. 1 and 3②) has been investigated for a better understanding of its photolysis and to inform future reaction design. Employing nanosecond pulsed laser irradiation, the wavelength was tuned. Conversion, X_4 , and yield, Y_4 , were then followed by tracking the

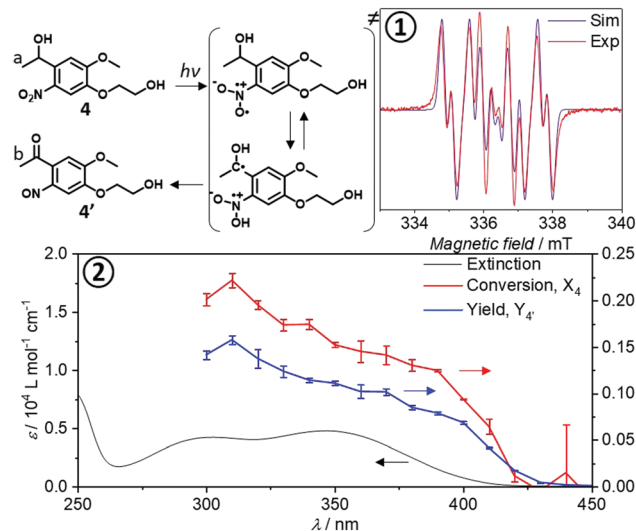


Fig. 3 ① Simulated and experimental electron paramagnetic resonance (EPR) spectra of the *o*NB-dialcohol in CDCl_3 at ambient temperature and the proposed radical formation. ② Action plot of compound **4** in acetonitrile, indicating the conversion from **4** to **4'**, X_4 , depicted in red and the yield Y_4 in blue, while the extinction coefficient of compound **4** as a function of wavelength is provided in black.

protons a and b via $^1\text{H-NMR}$ spectroscopy (Fig. 3② and Fig. S22, ESI†). The action plot of compound **4** is displayed in (Fig. 3②) along with the evolution of its extinction coefficient as a function of wavelength. Interestingly, the degradation product shows a peak at 310 nm which is not related to the absorption maximum (λ_{max} close to 350 nm). While the *o*NB dialcohol shows no significant absorption around 400 nm, degradation is still taking place until 425 nm, where the absorption is below the detection limit. Further, a gap between the conversion and yield was found which remained constant until 425 nm. Indeed, given the fact that the formation of **4'** is consistently less efficient than the photolysis of the *o*NB dialcohol, the selectivity of this reaction can be estimated. Additionally, a similar kinetic study using LEDs ranging from 340 to 415 nm was conducted, thus allowing to access the degradation performance of the compound **4** with a more accessible method (Fig. S17–S20, ESI†).

Pulsed-Laser-Degradation hyphenated Size Exclusion Chromatography (PLD-SEC) enables the direct control of polymers photolysis with a precise number of photons. Although the degradation efficiency of the *o*NB dialcohol subsides continuously throughout the blue visible region (Fig. 1), an irradiation wavelength of 365 nm was chosen in order to balance degradation efficiency and glass absorption. In a first approach, the photolysis experiments were performed in solution in THF, using the polymers previously synthesized (Scheme 1 and Fig. 2). As shown in Fig. 2 (purple dotted lines), a significant shift towards higher elution times (lower molecular weights) is observed. We assume that the heterolytic C–O bond fission involving the radicals observed via EPR (Fig. 3①, Scheme S3 and Fig. S21, ESI† for further details) leads to the formation of fragments as depicted in Fig. S25 (ESI†). Further, the photolysis of *o*NB-based PU was performed on thin films using 10 μL of a 7 $\mu\text{g mL}^{-1}$ polymer solution in dioxane or DMSO. The

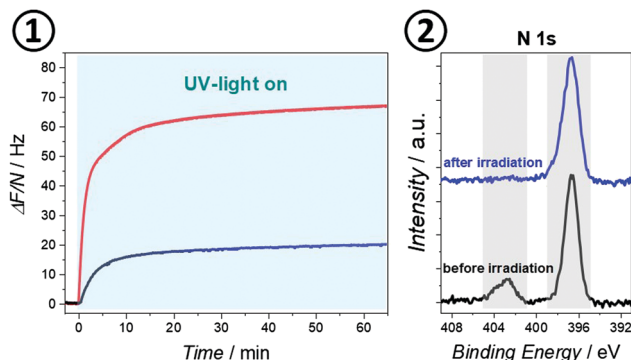


Fig. 4 ① Frequency change of quartz crystal coated with 10 μL of a 7 $\mu\text{g mL}^{-1}$ polymer solution (PU-20 min) in dioxane (red) and DMSO (blue) and irradiated with a 365 nm LED from t_0 . Data obtained using a quartz crystal microbalance at 25 $^\circ\text{C}$ with a constant flow of water. ② X-ray photoelectron spectroscopy of a silica slide coated with 10 μL of a 7 $\mu\text{g mL}^{-1}$ polymer solution (PU-20 min) in DMSO, irradiated with a 365 nm LED and washed out with water. Wide scans are available in the ESI,† Fig. S27.

thickness was assessed using ellipsometry and found to be of ~ 10 nm (for the DMSO). The photolysis of PU in thin films was assessed by performing *in situ* Quartz Crystal Microbalance (QCM) measurements employing a window module and a 365 nm LED (Fig. 4①) with a constant flow of water ($100 \mu\text{L min}^{-1}$). The resonance frequency of the quartz sensor is influenced by the addition or removal of mass onto the electrode. Indeed, the increase of averaged resonance frequencies upon light irradiation demonstrate a significant loss of material on the surface of the crystal. Due to an increased thickness of the dioxane spin-coated sample, a greater overall mass change was detected. In addition, X-ray photoelectron spectroscopy (XPS) was chosen to assess the chemical changes on the thin film before and after UV-irradiation (365 nm). The high-resolution spectrum of the nitrogen N 1s binding energies suggests that the urethane linkage remains intact after photolysis with the presence of N–C bonds (397 eV) before and after both light irradiation (Fig. 4②). Additionally, the loss of NO₂ functions (403 eV) after photolysis suggests that the *o*NB undergoes photocleavage.

In summary, we demonstrate the photodegradability of polyurethanes in solution as well as in thin films. The formation of linear polyurethanes bearing *o*NB moieties was performed via step-growth polymerization ensuring the presence of a cleaving point after every second monomer unit, as proven with high resolution mass spectrometry. The in-depth study of the photodegradability of the *o*NB-comonomer and linear PU in solution allowed for a better understanding of the expected chemical functions on the thin film after photolysis. The degradation of PU was successful both in solution and in thin films as demonstrated with thin film analysis using XPS and QCM.

C. B.-K., J. B., E. B. and A.-N. U. gratefully acknowledge financial support from the Australian Research Council (ARC) and the company Ivoclar Vivadent (Liechtenstein) for key funding in the context of the Linkage Grant LP170100979. The authors acknowledge the facilities and the scientific and

technical assistance at the Central Analytical Research Facility (CARF) operated by the Institute for Future Environments (IFE).

Conflicts of interest

There are no conflicts to declare.

Notes and references

- Z. Li, R. Zhang, K.-S. Moon, Y. Liu, K. Hansen, T. Le and C. P. Wong, *Adv. Funct. Mater.*, 2013, **23**, 1459–1465.
- M. R. Patel, J. M. Shukla, N. K. Patel and K. H. Patel, *Mater. Res.*, 2009, **12**, 385–393.
- G. Ciardelli, A. Rechichi, P. Cerrai, M. Tricoli, N. Barbani and P. Giusti, *Macromol. Symp.*, 2004, **218**, 261–272.
- M. Nouman, E. Jubeli, J. Saunier and N. Yagoubi, *J. Biomed. Mater. Res., Part A*, 2016, **104**, 2954–2967.
- B. D. Ratner, K. W. Gladhill and T. A. Horbett, *J. Biomed. Mater. Res.*, 1988, **22**, 509–527.
- L. Zhou, D. Liang, X. He, J. Li, H. Tan, J. Li, Q. Fu and Q. Gu, *Biomaterials*, 2012, **33**, 2734–2745.
- L. Zhou, L. Yu, M. Ding, J. Li, H. Tan, Z. Wang and Q. Fu, *Macromolecules*, 2011, **44**, 857–864.
- Z. Wang, P. Wan, M. Ding, X. Yi, J. Li, Q. Fu and H. Tan, *J. Polym. Sci., Part A: Polym. Chem.*, 2011, **49**, 2033–2042.
- O. Bayer, *Angew. Chem.*, 1947, **59**, 257–288.
- S. Awasthi and D. Agarwal, *J. Coat. Technol. Res.*, 2007, **4**, 67–73.
- D. K. Schneiderman, M. E. Vanderlaan, A. M. Mannion, T. R. Panthani, D. C. Batiste, J. Z. Wang, F. S. Bates, C. W. Macosko and M. A. Hillmyer, *ACS Macro Lett.*, 2016, **5**, 515–518.
- W. Yang, Q. Dong, S. Liu, H. Xie, L. Liu and J. Li, *Procedia Environ. Sci.*, 2012, **16**, 167–175.
- D. R. Griffin and A. M. Kasko, *J. Am. Chem. Soc.*, 2012, **134**, 13103–13107.
- P. Klán, T. Šolomek, C. G. Bochet, A. Blanc, R. Givens, M. Rubina, V. Popik, A. Kostikov and J. Wirz, *Chem. Rev.*, 2013, **113**, 119–191.
- K. J. R. Lewis, M. W. Tibbitt, Y. Zhao, K. Branchfield, X. Sun, V. Balasubramaniam and K. S. Anseth, *Biomater. Sci.*, 2015, **3**, 821–832.
- L. Li, X.-X. Deng, Z.-L. Li, F.-S. Du and Z.-C. Li, *Macromolecules*, 2014, **47**, 4660–4667.
- A. M. Rosales, S. L. Vega, F. W. DelRio, J. A. Burdick and K. S. Anseth, *Angew. Chem., Int. Ed.*, 2017, **56**, 12132–12136.
- O. Bertrand, J.-M. Schumers, C. Kuppan, J. Marchand-Brynaert, C.-A. Fustin and J.-F. Gohy, *Soft Matter*, 2011, **7**, 6891–6896.
- J.-M. Schumers, O. Bertrand, C.-A. Fustin and J.-F. Gohy, *J. Polym. Sci., Part A: Polym. Chem.*, 2012, **50**, 599–608.
- B. Yan, J.-C. Boyer, N. R. Branda and Y. Zhao, *J. Am. Chem. Soc.*, 2011, **133**, 19714–19717.
- H. Zhao, W. Gu, E. Sterner, T. P. Russell, E. B. Coughlin and P. Theato, *Macromolecules*, 2011, **44**, 6433–6440.
- H. Zhao, E. S. Sterner, E. B. Coughlin and P. Theato, *Macromolecules*, 2012, **45**, 1723–1736.
- M. Kyrish, U. Utzinger, M. R. Descour, B. K. Baggett and T. S. Tkaczyk, *Opt. Express*, 2011, **19**, 7603–7615.
- P. L. Kolker and W. A. Waters, *J. Am. Chem. Soc.*, 1964, 1136–1141.
- V. Jagannadham and S. Steenken, *J. Am. Chem. Soc.*, 1984, **106**, 6542–6551.
- E. T. Strom and J. Weinstein, *J. Org. Chem.*, 1967, **32**, 3705–3706.
- J. E. T. Corrie, B. C. Gilbert, V. R. N. Munasinghe and A. C. Whitwood, *J. Am. Chem. Soc.*, 2000, 2483–2491.
- D. E. Fast, A. Lauer, J. P. Menzel, A.-M. Kelterer, G. Gescheidt and C. Barner-Kowollik, *Macromolecules*, 2017, **50**, 1815–1823.
- J. P. Menzel, B. B. Noble, A. Lauer, M. L. Coote, J. P. Blinco and C. Barner-Kowollik, *J. Am. Chem. Soc.*, 2017, **139**, 15812–15820.
- B. T. Tuten, J. P. Menzel, K. Pahnke, J. P. Blinco and C. Barner-Kowollik, *Chem. Commun.*, 2017, **53**, 4501–4504.